Copyright Warning & Restrictions

The copyright law of the United States (Title 17, United States Code) governs the making of photocopies or other reproductions of copyrighted material.

Under certain conditions specified in the law, libraries and archives are authorized to furnish a photocopy or other reproduction. One of these specified conditions is that the photocopy or reproduction is not to be "used for any purpose other than private study, scholarship, or research." If a, user makes a request for, or later uses, a photocopy or reproduction for purposes in excess of "fair use" that user may be liable for copyright infringement,

This institution reserves the right to refuse to accept a copying order if, in its judgment, fulfillment of the order would involve violation of copyright law.

Please Note: The author retains the copyright while the New Jersey Institute of Technology reserves the right to distribute this thesis or dissertation

Printing note: If you do not wish to print this page, then select "Pages from: first page # to: last page #" on the print dialog screen

FINITE ELEMENT ANALYSIS OF THE FEMORAL HEAD

by
GHANDIKOTA RAMAMURTHY

Thesis submitted to the Faculty of the Graduate School
of the New Jersey Institute of Technology in Partial fulfillment
of the requirements for the degree of
Master of Science in Mechanical Engineering
1983

APPROVAL SHEET

Title of Thesis: Finite element analysis of the Femoral Head

Name of Candidate : Ghandikota Ramamurthy

Thesis and Abstract Approved :

Prof. M. Pappas Date
Professor
Mechanical Engineering Dept.

Prof. H. Herman Date
Professor
Mechanical Engineering Dept.

Prof. B. Koplik Date
Professor
Mechanical Engineering Dept.

VITA

Name : Ghandikota Ramamurthy

Degree and date to be conferred: M.S.M.E., 1983

Secondary education: Hijli high school, May 1976

Collegiate institutions attended	Dates	Degree	Date of Degree
New Jersey Inst. of Tech.	9/81-9/83	M.S.M.E.	Oct 1983
R.E.C., Durgapur, India	7/76-6/81	B.E.M.E.	June 1981

Major: Mechanical Engineering

Publications: Elipsograph, Invention intelligence, March 1981, pp 129-130, N.R.D.C., India

Positions held: Graduate Assistant, M.E. Dept., N.J.I.T.

ABSTRACT

Title of thesis: Finite element analysis of the Femoral Head

Ghandikota Ramamurthy, M.S.M.E.,1983

Thesis directed by: Professor M. Pappas

Femoral component loosening and prosthetic stem fractures have renewed interest in conservative alternatives to conventional total hip replacements. One such alternative is the concept of surface replacement. The objective in this study is a finite element analysis of a femoral surface replacement cup with particular attention given to the interfacial stresses. An axisymmetric model with a grid of two-dimensional isoparametric elements is generated. This study utilizes an adaptive model so as to include the effect of bone remodeling in response to stress. The stiffness is considered to be linearly proportional to the stress in the femoral head and neck. Isotropic properties are chosen. The stresses are determined by performing iterative finite element analyses based upon an appropriate variation of the stiffness property in each analysis until the results obtained are within the convergence limit. Plots of stress contours in the femoral head are obtained for the loads acting on the joint during walking.

PREFACE

The finite element analysis has wide applications in biomaterial and biomechanics research. The analysis of the surface replacement of the femoral head is considered to provide an insight to a better design of the hip joint replacement. The present study makes use of the GIFTS 5.06 software. However, the scope of the investigation is limited due to the unavailability of the software on the computer resources available for the research. Details of the initial preparation for the model set up and generation are presented here so that the reader is at ease to develop and analyze the model to obtain the results. Even though the emphasis is on the GIFTS software yet the reader is at no loss to perform the analysis using any other software which supports the analysis of axisymmetric solids subjected to non- axisymmetric loading, eg., ANSYS software.

ACKNOWLEDGEMENT

I take the opportunity to record my sincerest gratitude to Professor Michael Pappas, Mechanical Engineering Department of NJIT for his benevolence, active interest, and valuable guidance throughout the course of this thesis work. It was a priviledged pleasure to work under the guidance of my esteemed Professor.

I am extremely thankful to Mr. Robert R. Pescinski, Academic Computing Services, for the help he gave in installing the GIFTS software. I also express my indebtness to Professor Harry Herman, Graduate Advisor, and to Professor Bernard Koplik, Chairman of the Mechanical Engineering Department for their help and encouragement given.

G. Ramamurthy

TABLE OF CONTENTS

LIST OF TABLES

LIST OF FIGURES

1) INTRODUCTION TO SURFACE REPLACEMENT

A) NEED FOR SURFACE REPLACEMENT

Most of the total hip arthroplasties are performed on joints which have been disorganised by osteoarthrosis or rheumatoid arthritis. The natural histories of these two complaints differ and also the states of joints considered for replacement differ in some respects which need to be considered in prostheses design. In general the affected joint will exhibit some combination of pain, stiffness, deformity and instability. From a survey of total hip replacements performed at the Hospital for Special Surgery, New York City during the period 1971 to 1977 it was found that out of approximately 3000 surgeries there were 35 cases of mechanical failures in absence of infection. Of these 35 cases, 14 patients had dislocations of the prostheses and 7 patients had loosening of the femoral component. Besides these 6 patients had fractures of the femoral stem and 3 patients had loosening of the acetabular component[ref.1].

A similar survey done by Beckenbaugh and Ilstrup[ref.2] shows that out of 333 consecutive charnley total hip arthroplasties, 24% of the replacements gave roentgenographic evidence of loosening of the femoral component. The above mentioned facts show high incidences of component loosening and femoral stem fractures.

The goals of hip reconstruction are

1) to eliminate or reduce pain,

2) to restore normal activity and

3) to increase stability.

Pain can be relieved provided all surgical components of the prostheses -cement- bone reconstruction are properly implanted and remain structurally sound. The life of the replacement can be increased if the stresses in the components are below the allowable limits.

Even though total hip replacement has proved to be a reliable method for relieving pain and restoring joint function by proper fixation, yet femoral fractures and loosening suggests alternatives to conventional total hip arthroplasty. One such alternative is to limit the extent of early surgical intervention by resurfacing the femoral head and acetabulum, while maintaining vascularization of the femoral head. This is the concept of surface replacement[ref.3].

B) ADVANTAGES AND SALIENT FEATURES

Immediate advantages and salient features of the surface replacement are the following :

a) It eliminates the possibility of stem loosening, migration and stem fatigue fracture.

b) Stemless resurfacing devices may eliminate long-term fixation problems which apparently result from elastic mismatch between the stem and the femoral shaft.

c) It requires minimal resection of femoral bone tissue and is thus more conservative.

d) The hip can be resurfaced without interfering with the abductor muscles and without removing healthy bone.

e) In total hip replacements deep infection rates of about 1-8% occurs, which is a serious problem. Surface replacement reduces the possibility of deep bone infection associated with the invasion of the medullary canal.

f) Surface replacement can maintain normal weight bearing structure of the proximal femur.

g) Here more load bearing bone is retained. This is critical in maintaining the viability of the femoral head/neck and in reducing the likelihood of the femoral neck fractures.

h) Since minimal bone is removed in surface replacement therefore surface replacement allows for revision to a stem type prostheses for a proper functioning of the joint. In the extreme event of the failure of the device fusion process can be performed.

i) Besides the above advantages, surface replacement devices can be implanted in younger patients with good reliability.

C) MODEL ANALYSIS

The purpose of this study is to investigate the femoral surface replacement component. The emphasis is on the interfacial stresses of the prostheses and the bone

adjacent. A uniform state of stress is desired to the extent possible. To prevent loosening of the component tensile stresses must be avoided. The objective is to make the prostheses suitable for adaptation by performing an analysis so as to have as far as possible a uniform state of compressive stress by minimising the shear and tensile stresses. The loads on the component and the stresses in it can be obtained from a proper analysis of the joint. Theoretical stress analysis of the composite prostheses -cement- bone structure holds considerable promise for a better understanding of the mechanical behaviour.

The model analysis is complex in nature because of the

1) three-dimensional geometry ,

2) non-homogeneous, non-linear and anisotropic properties of the cancellous and cortical bone architecture and

3) dynamic loading configuration from muscle force and joint reactions produced by various human activities.

Analytical solutions are possible for problems having simple geometry and simplified external loading configurations. The stress analysis in a solid body involves the solution of a set of mathematical equations which govern the behaviour of the material subjected to mechanical loading. However, geometric irregularities and material non-uniformity in the femoral head make these analytical solutions impractical. One can make simplified

assumptions but these may effect the reality of the model. One such stress analysis on the femoral shaft is presented by Koch (1917) [ref.4] using simple equations of strength of materials.

An alternative to the classical analytical methods is to utilise approximation techniques involving computer and numerical analysis. The most widely used among these methods is the finite element analysis using high speed digital computers to perform a very large number of matrix operations [ref.5,6].

2) FINITE ELEMENT ANALYSIS TECHNIQUE

A) GENERAL METHOD :

The finite element analysis is a numerical technique in which a structural part is divided into small but finite elements. These elements are then superimposed on to a grid system, where identifiable points of the elements, called nodes, are referenced with respect to a co-ordinate system.

Since the variation of the field variable (like diplacement, stress, temperature, pressure, etc) inside the continuum is not known the variation in the element is approximated by simple functions defined in terms of the values of the field variable at the nodes. These interpolating functions are called shape functions. The solution of the field equations yield the nodal values of the field variable. Once these are known, the shape functions define the field variable throughout the assemblese of the elements. The following are the general steps in a finite element analysis [ref.5,6]:

The first step, as mentioned above, is the discretization of the region into elements. The region that is being analyzed is modelled with appropriate finite elements, i.e., the number, size & shape and arrangement of the elements has to be decided.

The second step is the selection of a proper interpolation function to approximate the unknown solution.

The assumed solution should be simple and satisfy certain convergence requirements. The displacement model within an element may be assumed as

$$\{U\} = [u, v, w]^T = [N]\{Q\} \qquad (1)$$

where {U} is the vector of nodal displacements u, v and w, and { Q } is the nodal displacement degrees of freedom of the element and [N] is the matrix of shape functions.

The next step is the derivation of the element stiffness matrices and load vectors from the assumed displacement model using either equilibrium equations or variational formulation methods. The equilibrium equations can be derived using different methods like force method, displacement method, etc. Examples of variational formulation methods are the principle of minimum potential energy, principle of minimum complementary energy, etc.

The derivation using the principle of minimum potential energy is as follows [ref.5]:

If Π_p = the potential energy of the body, and

E = total number of elements then

$$\Pi_p = \sum_{e=1}^{E} \Pi_p^{(e)} \qquad (2)$$

where $\Pi_p^{(e)}$ is the potential energy of the element, e,

given by

$$\Pi_p^{(e)} = \frac{1}{2}\iiint_{V^{(e)}} [\epsilon]^T [D] (\{\epsilon\} - 2\{\epsilon_0\})\, dV$$
$$- \iint_{S_1^{(e)}} [U]^T \{\bar{\Phi}\}\, dS_1$$
$$- \iiint_{V^{(e)}} [U]^T \{\phi\}\, dV \qquad (3)$$

where

$V^{(e)}$ = volume of the element

$S_1^{(e)}$ = surface region over which distributed surface forces are prescribed

$\{\bar{\Phi}\}$ = surface forces vector

$\{\phi\}$ = body forces (per unit volume) vector

$\{\epsilon\}$ = strain vector

$\{\epsilon_0\}$ = initial strain vector

$[D]$ = material property matrix

Considering linear isotropic 3-D solid element,

$$[D] = \frac{E}{(1+\nu)(1-2\nu)} \begin{bmatrix} 1-\nu & \nu & \nu & 0 & 0 & 0 \\ \nu & 1-\nu & \nu & 0 & 0 & 0 \\ \nu & \nu & 1-\nu & 0 & 0 & 0 \\ 0 & 0 & 0 & \frac{1-2\nu}{2} & 0 & 0 \\ 0 & 0 & 0 & 0 & \frac{1-2\nu}{2} & 0 \\ 0 & 0 & 0 & 0 & 0 & \frac{1-2\nu}{2} \end{bmatrix} \qquad (4)$$

The strain vector $\{\epsilon\}$ can be expressed in terms of the nodal displacement vector $\{q^{(e)}\}$ as follows:

$$\{\epsilon\} = \begin{Bmatrix} \epsilon_{xx} \\ \epsilon_{yy} \\ \epsilon_{zz} \\ \epsilon_{xy} \\ \epsilon_{yz} \\ \epsilon_{zx} \end{Bmatrix} = \begin{Bmatrix} \frac{\partial u}{\partial x} \\ \frac{\partial v}{\partial y} \\ \frac{\partial w}{\partial z} \\ \frac{\partial u}{\partial y} + \frac{\partial v}{\partial x} \\ \frac{\partial v}{\partial z} + \frac{\partial w}{\partial y} \\ \frac{\partial w}{\partial x} + \frac{\partial u}{\partial z} \end{Bmatrix} = \begin{bmatrix} \frac{\partial}{\partial x} & 0 & 0 \\ 0 & \frac{\partial}{\partial y} & 0 \\ 0 & 0 & \frac{\partial}{\partial z} \\ \frac{\partial}{\partial y} & \frac{\partial}{\partial x} & 0 \\ 0 & \frac{\partial}{\partial z} & \frac{\partial}{\partial y} \\ \frac{\partial}{\partial z} & 0 & \frac{\partial}{\partial x} \end{bmatrix} \begin{Bmatrix} u \\ v \\ w \end{Bmatrix}$$

$$= [B]\{q^{(e)}\} \qquad (5)$$

where

$$[B] = \begin{bmatrix} \frac{\partial}{\partial x} & 0 & 0 \\ 0 & \frac{\partial}{\partial y} & 0 \\ 0 & 0 & \frac{\partial}{\partial z} \\ \frac{\partial}{\partial y} & \frac{\partial}{\partial x} & 0 \\ 0 & \frac{\partial}{\partial z} & \frac{\partial}{\partial y} \\ \frac{\partial}{\partial z} & 0 & \frac{\partial}{\partial x} \end{bmatrix} [N] \qquad (6)$$

The stress $\{\sigma\}$ can be obtained from the strains $\{\epsilon\}$ by the relation

$$\{\sigma\} = [D](\{\epsilon\} - \{\epsilon_0\})$$

$$= [D][B]\{q^{(e)}\} - [D]\{\epsilon_0\} \qquad (7)$$

Substituting for $\{U\}$ and $\{\epsilon\}$ the equation for potential energy becomes

$$\Pi_p^{(e)} = \frac{1}{2}\iiint_{V^{(e)}} [q^{(e)}]^T [B]^T [D][B]\{q^{(e)}\}\, dV$$
$$-\frac{1}{2}\iiint_{V^{(e)}} [q^{(e)}]^T [B]^T [D]\{\epsilon_0\}\, dV$$
$$-\iint_{S_1^{(e)}} [q^{(e)}]^T [N]^T \{\bar{\phi}\}\, dS_1$$
$$-\frac{1}{2}\iiint_{V^{(e)}} [q^{(e)}]^T [N]^T \{\phi\}\, dV \qquad (8)$$

So far the potential energy is calculated considering only body and surface forces. However, in general some external concentrated forces act at various nodes. If $\{P_c\}$ be the nodal forces and $\{Q\}$ the corresponding displacements of the entire region, then the total potential energy is given by

$$\Pi_p = \sum_{e=1}^{E} \Pi_p^{(e)} - [Q]^T [P_c] \qquad (9)$$

where

$$\{Q\} = [Q_1 \;\; Q_2 \;\; \ldots \;\; Q_M]^T \qquad (10)$$

the nodal displacements of the whole region and M is the total number of degrees of freedom.

Considering the summation over all elements, i.e., using global relations the total potential energy of the region in terms of the nodal degrees of freedom, $\{Q\}$ is given by

$$\Pi_p = \frac{1}{2}[Q]^T\left[\sum_{e=1}^{E}\iiint_{V^{(e)}}[B]^T[D][B]\,dV\right]\{Q\}$$

$$-[Q]^T\sum_{e=1}^{E}\left(\iiint_{V^{(e)}}[B]^T[D]\{\epsilon_0\}\,dV\right.$$

$$\left.+\iint_{S_1^{(e)}}[N]^T\{\bar{\Phi}\}\,dS_1+\iiint_{V^{(e)}}[N]^T\{\phi\}\,dV\right)$$

$$-[Q]^T\{P_c\} \qquad (11)$$

The necessary conditions for minimization of

of potential energy are

$$\frac{\partial \Pi_p}{\partial Q_1}=\frac{\partial \Pi_p}{\partial Q_2}=\cdots=\frac{\partial \Pi_p}{\partial Q_M}=0 \qquad (12)$$

$$\text{i.e.,}\quad \frac{\partial \Pi_p}{\partial \{Q\}}=\{0\} \qquad (13)$$

Using eqns 11 & 13 one obtains the followins

$$\left[\sum_{e=1}^{E} \iiint_{V^{(e)}} [B]^T [D] [B] \, dV \right] \{Q\}$$

$$= \{P_c\} + \sum_{e=1}^{E} \left(\iiint_{V^{(e)}} [B]^T [D] \{\epsilon_0\} \, dV \right.$$

$$\left. + \iint_{S_1^{(e)}} [N]^T \{\bar{\phi}\} \, dS_1 + \iiint_{V^{(e)}} [N]^T \{\phi\} \, dV \right) \quad (14)$$

i.e.,

$$\left(\sum_{e=1}^{E} [K^{(e)}] \right) \{Q\} = \{P_c\} + \sum_{e=1}^{E} \left(\{P_i^{(e)}\} + \{P_s^{(e)}\} + \{P_b^{(e)}\} \right)$$

$$= \{P\} \quad (15)$$

where

$$[K^{(e)}] = [B]^T [D] [B] \, dV \quad (16)$$

= element stiffness matrix

$$\{P_i^{(e)}\} = \iiint_{V^{(e)}} [B]^T [D] \{\epsilon_o\} \, dV \qquad (17)$$

= element load vector due to initial strains

$$\{P_s^{(e)}\} = \iint_{S_1^{(e)}} [N]^T \{\bar{\phi}\} \, dS_1 \qquad (18)$$

= element load vector due to surface forces

$$\{P_b^{(e)}\} = \iiint_{V^{(e)}} [N]^T \{\phi\} \, dV \qquad (19)$$

= element load vector due to body forces

$\{P\}$ = total load vector

Once the stiffness matrix for each element has been derived the next step is the assemblage of the element equations to obtain the overall equilibrium equations as given by

$$[K]\{Q\} = \{P\} \qquad (20)$$

$$\text{where } [K] = \sum_{e=1}^{E} [K^{(e)}] \qquad (21)$$

= global stiffness matrix

$$\{P\} = \{P_C\} + \sum_{e=1}^{E} \{P_i^{(e)}\} + \sum_{e=1}^{E} \{P_s^{(e)}\} + \sum_{e=1}^{E} \{P_b^{(e)}\} \qquad (22)$$

= nodal force vector

$\{Q\}$ = nodal displacements vector

The next step is the determination of the solution for the unknown displacements. In linear equilibrium problems, there is a relatively straight forward application of matrix algebra techniques. However, for non-linear problems the desired solutions are obtained by a sequence of steps, each step involving the modification of the stiffness matrix and/or load vector. Once the displacement matrix is determined, the strains can be evaluated from the strain-displacement relations and the stresses can be evaluated from the stress - strain relations.

B) AXISYMMETRIC ANALYSIS :

In the present study the structural components are axisymmetric or approximately axisymmetric. The stress distribution in the structure is 3-Dimensional and could be

calculated using a 3-D finite element idealization. However, taking advantage of the axisymmetric geometry and the exact loadings applied, the computational effort can be reduced significantly. In the ideal case the loading is also axisymmetric and in such a situation a 2-D analysis of a unit radian of the structure yields the complete stress and strain distributions. However, if the axisymmetric model is subjected to non- axisymmetric loadings then the choice lies between a fully 3-D analysis, in which substructuring or cyclic symmetry are used, and a fourier decomposition of the loads with a fourier axisymmetric solution.

The following gives an insight into the analysis of an axisymmetric model subjected to non- axisymmetric loadings in the radial and axial directions using a triangular (3 -node) axisymmetric element with the loadings represented as a superposition of the fourier components[ref.6]. Analysis of the radial loading is presented here. Similar analysis of the axial loadings can be performed and the two loadings are combined together to get the solution for the resultant loadings.

In the analysis the external radial loadings $R_r(\theta, z)$ (cf.figure 1) is expanded in the fourier series

$$R_r = \sum_{p=1}^{p_c} R_{pc} \cos p\theta + \sum_{p=1}^{p_s} R_{ps} \sin p\theta \quad (23)$$

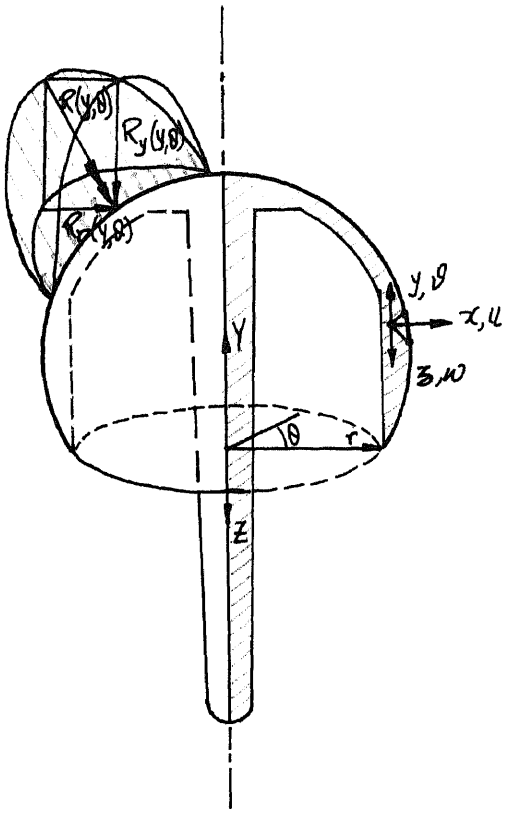

3-NODE ELEMENT

u - radial displ.
v - axial displ.
w - circum. displ.

AXISYMMETRIC MODEL
SURFACE REPLACEMENT CUP

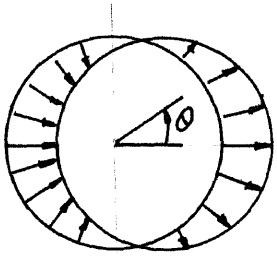

1ST SYMMETRIC LOAD TERM

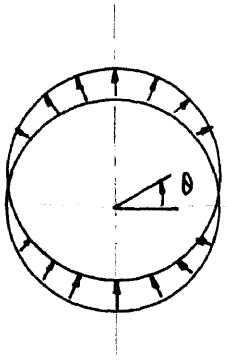

1ST ANTISYMMETRIC LOAD TERM

REPRESENTATION OF NON-AXISYMMETRIC LOADING

FIGURE 1

where P_C and P_S are the total number of symmetric and antisymmetric load contributions, about $\theta = 0$ respectively. The response due to the symmetric and antisymmetric load contributions are superimposed to yield the complete analysis.

Considering the response due to symmetric loading one has for an element,

$$u(x,y,\theta) = \sum_{p=1}^{P_c} \cos p\theta \; [N] \; u^p \qquad (24)$$

$$v(x,y,\theta) = \sum_{p=1}^{P_c} \cos p\theta \; [N] \; v^p \qquad (25)$$

$$w(x,y,\theta) = \sum_{p=1}^{P_c} \cos p\theta \; [N] \; w^p \qquad (26)$$

where u^p, v^p, w^p are the element unknown generalized nodal point displacements corresponding to mode p.

The strains in cylindrical co-ordinates are

$$\{\epsilon\} = \begin{Bmatrix} \epsilon_{rr} \\ \epsilon_{yy} \\ \epsilon_{\theta\theta} \\ \gamma_{ry} \\ \gamma_{y\theta} \\ \gamma_{\theta r} \end{Bmatrix} \quad \begin{Bmatrix} \frac{\partial u}{\partial r} \\ \frac{\partial v}{\partial y} \\ \frac{u}{r} + \frac{1}{r} \cdot \frac{\partial w}{\partial \theta} \\ \frac{\partial u}{\partial y} + \frac{\partial v}{\partial r} \\ \frac{\partial w}{\partial y} + \frac{1}{r} \cdot \frac{\partial v}{\partial \theta} \\ \frac{\partial w}{\partial r} + \frac{1}{r} \cdot \frac{\partial u}{\partial \theta} - \frac{w}{r} \end{Bmatrix} \qquad (27)$$

Substituting eqns 24-26 into 27 one obtains the strain -displacement matrix, $[B_p]$, for each value of p and superimposing the strain distributions contained in each harmonic, the total strains are obtained. The unknown nodal point displacements can now be obtained using the equations 14-22 in the general procedure.

In a similar manner the response due to antisymmetric loading can be obtained simply by interchanging in eqns 24-26 all sine and cosine terms with cosine and sine terms respectively. Finally, the complete response of the model is obtained by superimposing the displacements corresponding to all harmonics.

3) SURVEY OF FEMORAL ANALYSIS

Application of finite element analysis to the stress analysis of human femur started in the early 70's. Different researchers presented different models using 2-D or 3-D elements and either considering or neglecting the side effects of muscle loadings in addition to the joint forces. Rybicki (1972) used a 2-D model considering muscle forces in addition to the joint forces and compared the results with those of simple beam theory. Brekelmans (1972) also used a 2-D model, considering muscle loading, with constant bone thickness and different loading conditions. Wood (1973) considered non-homogeneous properties and non-uniform thickness of the bone using 2-D isoparametric elements. He showed that the beam theory does not give accurate stress distribution for this case.

Application of finite element analysis of total hip replacement, i.e, considering both the prostheses and bone were presented by Andriacchi (1975), McNeice (1976), Forte (1975), Svensson (1977) and a few others. Their studies were mainly on the femoral stem discussing the stress patterns and the bone-cement interface studies.

Analysis using 3-D finite elements were done by Wood (1975), Olofsson (1976), Vallippan (1977), etc. However, their results were not accurate stress distributions and besides these models consumed a great amount of computation time for an analysis. Thus it does not seem realistic to

use such a model at present when a finer mesh of 2-D elements with varying thicknesses can show better results.

A comparative study of the different 2-D and 3-D element models was presented by Clarke, Gruen, Tarr and Sarmiento[ref.7] in the International conference proceedings on finite elements in biomechanics (feb '80). Their results are shown in table(I). Some of the finite element studies were directed towards the femoral head. One such presentation is by Brown and Fergusen[ref.8] using 2-D elements which could account for the non-uniform distribution of the stiffness in the cancellous bone. However, 2-D simulation of a 3-D problem does not give a true representation of the femoral head. Considering the femoral head, the prostheses and the bone adjacent is axisymmetric and the neck is approximately round. Thus in any event, since the interfacial stresses are under study here therefore a 2-D axisymmetric model closely resembles to the actual femoral head and the neck.

TABLE I. SURVEY OF F.E.A. MODELS

Study	Model	Element/ node	Femur	Femur +THR	Hip load(N)	Load axis(∅)(#)
Rybicki'7	2D-C	NS	X		2316	
Brekelmans'72	2D-NC	936/537	X		1200	20
Wood'73	2D-C	63/230(*)	P		1740	12
Simon'74	2D	168/129	P		804/2412	20
McNeice'76,'77	2D-C	897/982		X	2225	10,25(@)
Andriacchi'76	2D	NS		X	Jn	0,20,45(@)
Valliappan'77	3D	196/323(*)	P	X	790-11000	8(%)
Svensson'77	2D-C	118/NS	X	X	1620	24
Rohrle'77	3D	804/NS(*)	X	X	1716	16
Harris'78	3D	1232/815	X		2316	
Kwak'79	2D	152/NS		X	100	0,23,45(@)
Yettram'79	2D-B	751/834		X	1000	0
Crowninshield'79	3D	400/NS		X	Jn	20(%)
Tarr'79	3D	1032/1395(*)		X	Jn	20(@)

Note: Linear homogeneous isotropic model assumed unless otherwise specified.
B - orthrotropic model for cortical bone
C - composite model with out-of-plane geometries
Jn- normalized joint load; P- proximal femur
NC- no cancellous bone; NS- not specified; N- newtons
(#) - inclination to sagittal body plane (vertical)
(@) - inclination to lateral edge of stem
(%) - inclination to femoral shaft
(*) - only finest mesh noted

4) THE ADAPTIVE MODEL

It is observed from experimental studies that the bone remodels in response to the applied stress. The introduction of a prostheses produces a change in the stress distribution in the femoral head and neck since there is now a different composite structural stiffness.

According to Wolf's law the stiffness and strength vary with the stress applied. A linear relationship between the stiffness and strength is considered as follows

$$E = C\sigma \tag{28}$$

where E = chosen elastic stiffness,

C = constant of proportionality,

σ = stress resulting from applied load.

The constant of proportionality is determined from the yield strength and elastic modulus data obtained from the cancellous bone samples as presented by Brown et. al[ref.8]. Their studies show that the yield strength and the stiffness values are linearly proportional to one another, regardless of the testing direction. Considering the design stress to be approximately one-third of the yield strength, i.e.,

$$\sigma_{yp} \approx 3\sigma \ , \tag{29}$$

the constant, C, derived from the data in Brown et. al.[ref.8] is found to be 26.47 N per m^2/N per m^2. However, more experimental work need to be done to identify better

values of C.

To begin with the analysis, typical properties which are the result of the normal stress distribution are assumed. The introduction of the prostheses changes this distribution and thus the stiffness is changed in accordance with Wolf's law. Therefore, for the following analysis the stiffness is modified accordingly and the analysis repeated. This process is continued until convergence.

The following are the procedural steps in the adaptive model analysis:

1) An initial natural stiffness, E, is chosen in each element and σ is computed.

2) The stiffness distribution is modified by the relation

$$E^{r+1} = C\,\sigma^{r} \tag{30}$$

for each analysis r.

3) The results are checked for convergence, i.e., when

$$\left[\sum\left(E^{r+1} - E^{r}\right)^{2}\right]^{1/2} < \epsilon \tag{31}$$

is satisfied, where ϵ is an arbitrary convergence parameter, the analysis is terminated.

The final analysis and distribution are considered to be those associated with a fully remodeled femur.

5) OBJECTIVE OF PRESENT STUDY

The purpose of this study is to perform a finite element analysis of the adaptive femoral resurfacing cup model and analyze the stress distributions in the head due to the load transmitted from the acetabular region of the pelvis. The basic design requirements of cup arthroplasty to be followed are

1) adequate fixation of components; tensile and shear stresses are minimised to achieve a state of compressive stress,

2) selection of functional materials to provide both strength and wear,

3) proper fit of articular components i.e., the femoral cup with the acetabular cup.

Upon fulfilling these requirements the femoral head should remain (a) viable (after partial interruption of blood supply), (b) prove strong enough for resumed weight bearing and (c) have adequate fatigue resistance to withstand many years of cyclic loading.

The objective here is to study the interfacial stresses more specifically. To reduce the effect of disiusatrophy, a uniform state of stress in the bone is to be obtained as far as possible. High peak stresses should be avoided to minimise pressure neucrosis. To have a proper fixation without loosening, tensile stresses should be

avoided. Uniform compressive stress is ideal, shear stresses should be minimised and tensile stress zones should be removed as far as possible. Knowing the geometry and material properties, the objective here is to perform a finite element analysis to assess the degree of disiusatrophy and to achieve a uniform state of stress as possible. Once a particular state of stress is obtained in a finite element analysis, the stresses can be modified and reevaluated by performing a re- analysis varying the stiffness property in the prostheses -bone region. This process is repeated till the desired convergence limit is achieved.

The finite element model is constructed to consider all the above factors. The femoral cup is represented by a 2-D axisymmetric model using the solid mesh generation capabilities of GIFTS 5.06 . GIFTS is capable of solving axisymmetric models under either axisymmetric loads or non-axisymmetric loads broken down into a fourier series. Loads from joint reactions and muscle forces for common activities performed are taken from gross analytical models or from appropriate finite element model approximations as presented in the following sections.

6) THE ANATOMIC MODEL OF THE FEMORAL HEAD

For a successful mathematical model analysis of the femoral head replacement one needs to know the physiological model in detail. These studies have been split into three broad classifications as follows :

1) the shape or geometry of the femoral head ,

2) the material properties of the femoral head and

3) the boundary loading configuration on the femoral head during various activities.

A) GEOMETRY/SHAPE :

The shape and the inner architecture of the femoral head is well presented by Koch [ref.4]. The longitudinal sections are cut in planes parallel to the plane passing through the longitudinal axis of the shaft, head and neck of the femur, which is directed medially and about 12 degrees anterior to the true frontal plane of the body. Figure(2) shows one such section very close to the longitudinal axis of the bone. The inner architecture of the other parallel sections had a very close similarity to the one shown in figure(1). Figure(3) represents a sagittal section through the upper portion of the femur. This section includes the neutral plane of the upper femur and so gives one a good representation of the architecture of the femur in the region of the neutral axis. Figure 4 shows a series of tranverse sections (normal to the neutral axis) in the region of the femur head.

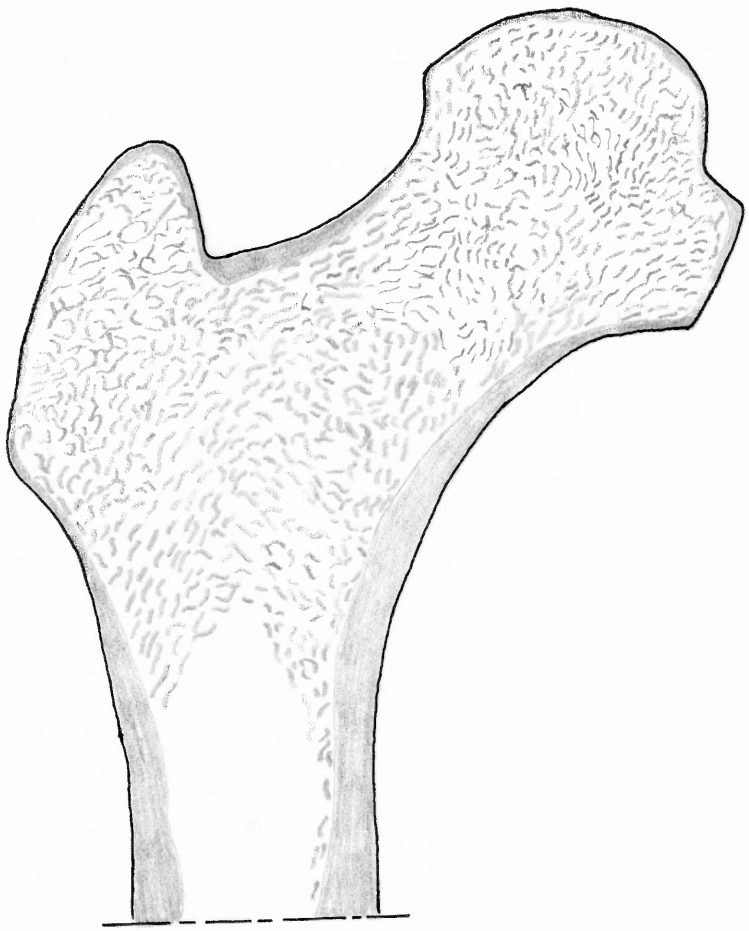

SPONGY BONE

COMPACT BONE

REF. NO. 4

FRONTAL LONGITUDINAL MID-SECTION OF UPPER LEFT FEMUR	SCALE 1:1
	FIGURE 2

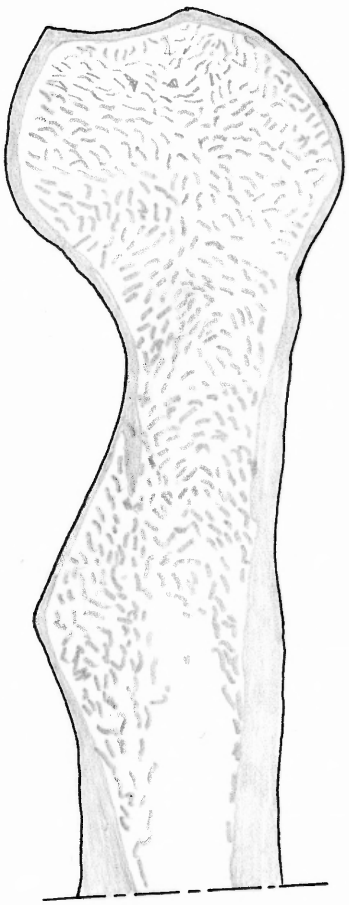

SPONGY BONE

COMPACT BONE

REF. NO. 4

SAGITTAL MID-SECTION OF UPPER FEMUR	SCALE 1:1
	FIGURE 3

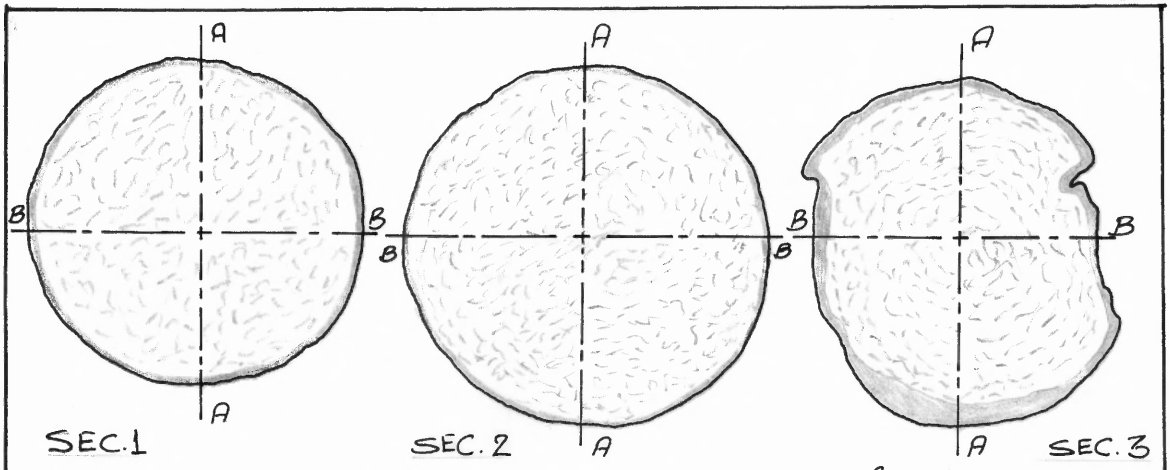

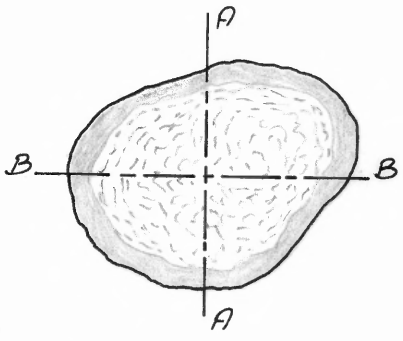

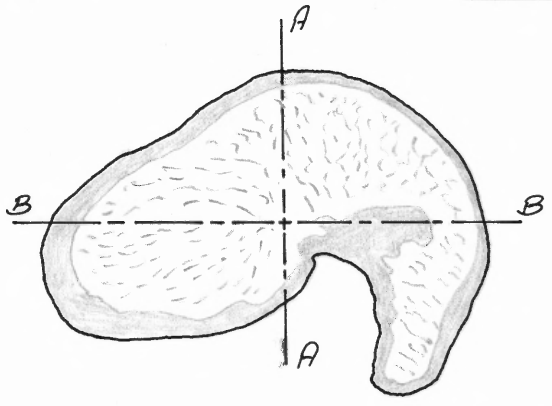

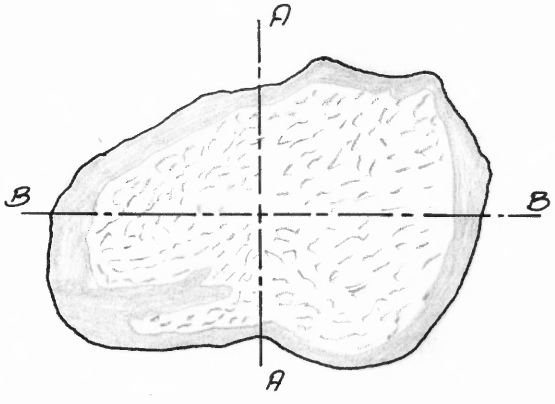

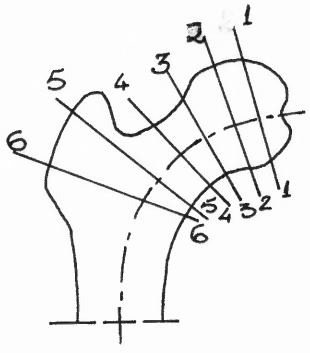

SPONGY BONE

COMPACT BONE

REF. NO. 4

TRANSVERSE SECTIONS IN UPPER FEMUR	SCALE 1:1
	FIGURE 4

Examining all these sections it is seen that the femoral head is made up entirely of the spongy bone except for a thin shell of compact bone forming the articular surface. The thinning of the trabeculae structure begins immediately below the atricular surface of the head. The transverse sections in the head are practically circular and these sections through the neck show a gradual thickening of the outer shell with a corresponding decrease in the density of the spongy bone as the sections are farther off from the head[cf. figure 4].

B) MATERIAL PROPERTIES :

Satisfactory material properties in the femoral head have been presented by Brown and Fergusen[ref.8]. They performed direct rheological tests for identifying the spatial and directional variatons of the mechanical properties of the cancellous bone in the human proximal femur. It is suggested by many authors that the stiffness and strength of the cancellous bone are immediately dependent upon the void fraction and the trabeculae pattern. Because of the complex internal anatomy, pronounced spatial and directional material properties may be expexted. So Brown and Ferguson made direct measurements to find the stiffness and strength of the individual cubic cancellous bone samples each undergoing successive uniaxial compressive loadings in the three mutually perpendicular directions. Based on the data from individual cubes from different locations within the femur head a computer contour routine and calcomp plotter were used to prepare the plots of the material property distributions of each section. The salient material property distributions for the present study are derived from the results of Brown and Ferguson.

There have been many investigators who have considered anistropic properties in the human femur. One such group are Bushkirk, Ashman and Cowin[ref.11]. They have developed an ultrasonic method to study the elastic

properties of the femur. The mean technical constants from their results are shown in table II.

S. Vallippan, S. Kjellberg and N. L. Svensson[ref.12] presented a comparison of the influence of isotropic and anisotropic properties on the stress distribution in the femur . Plots of maximum principal stress on the medial side and lateral side for the loading case for one-leg stance and walking are presented. Even though a comparison of the stress values on the medial side show some differences in the numerical values yet there has been no significant diffference on the lateral side. The deflections of the femoral head are found to be almost the same for both the isotropic and anisotropic cases. Since stresses are computed based on the deflections therefore there should be no large differences, for both the isotropic and anisotropic models, in stress values in the interfacial region of the prostheses. Besides there is not much cortical bone, which has high degree of anisotropic properties, left after resection. So to simplify the model isotropic material properties can be assumed for the present analysis.

As mentioned above the material properties of the femoral head are chosen from the results of Brown et. al.,[ref.8,13]. The model is subdivided into different regions based on the variation of material properties. Studying the variation of the elastic modulus and the yield

strength contours [cf. figure 5,6] in the femoral head, one finds that the properties are not truly axisymmetric. However, since these properties vary with growth therefore the material properties for the regions are chosen by judgement representing very closely the variations presented by Brown and Ferguson. The subdivisions and the properties of the different regions are illustrated in figure 7.

TABLE II. ANISOTROPIC PROPERTIES OF THE FEMUR

Young's modulii :

E_1 = 13.0 GPa E_2 = 14.4 GPa E_3 = 21.5 GPa

Risidity modulii :

G_{12} = 4.74 GPa G_{13} = 5.85 GPa G_{23} = 21.5 GPa

Poisson's ratio

μ_{12} = 0.37 μ_{13} = 0.24 μ_{23} = 0.22

μ_{21} = 0.42 μ_{31} = 0.40 μ_{32} = 0.33

Note: 1- radial direction

2- circumferential direction

3- longitudinal direction

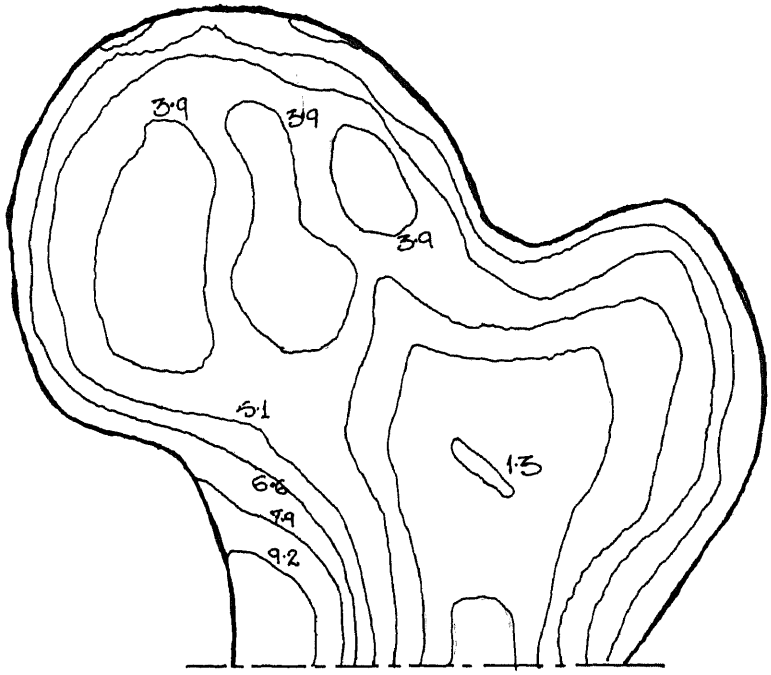

VALUES IN MULTIPLES OF 10^3 MN/M^2

CONTOURS FOR A CORONAL MID-SECTION

ELASTIC MODULUS VARIATIONS IN THE FEMORAL HEAD	REF. 8, 13
	FIGURE 5

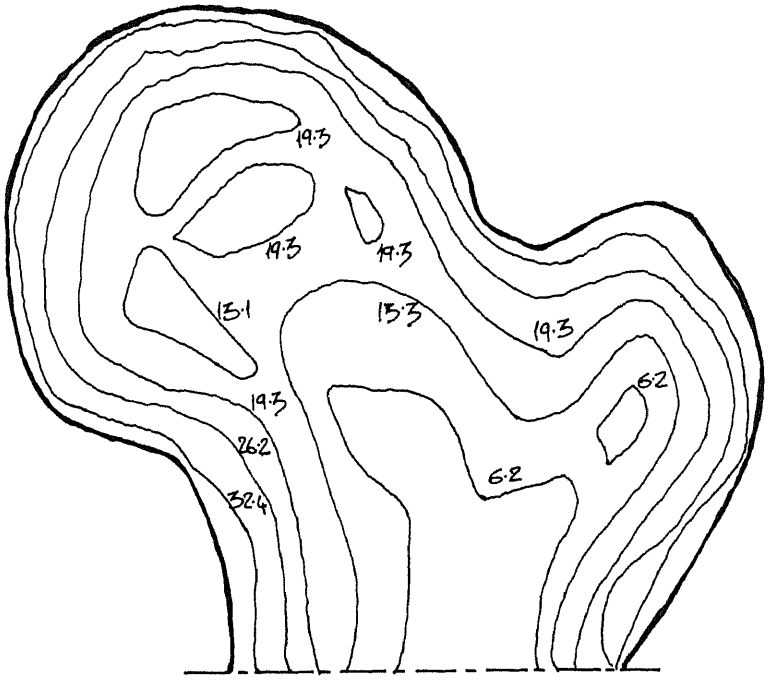

VALUES IN MULTIPLES OF 10 MN/M^2

CONTOURS FOR A CORONAL MID-SECTION

YEILD STRENGTH VARIATIONS IN THE FEMORAL HEAD	REF. 8, 13
	FIGURE 6

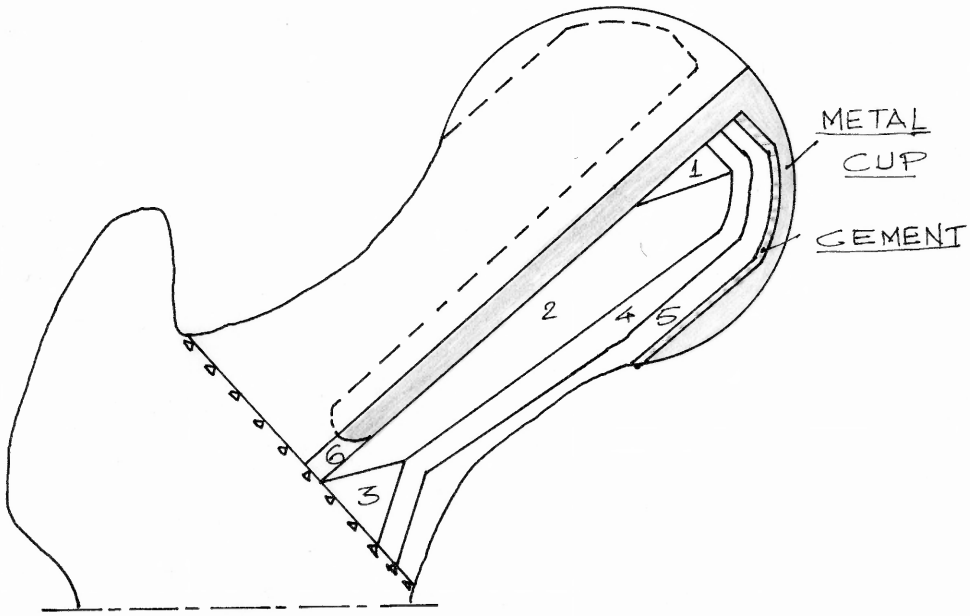

Region	E, MPa	$\sigma_{y.p.}$, MPa	μ
1, 4	6600	193	0·37
2	3900	131	0·37
3	5100	143	0·37
5	7900	262	0·42
6	1300	62	0·37

DERIVED MATERIAL PROPERTIES IN THE FEMORAL HEAD

REF. 8,13

FIGURE 7

C) BOUNDARY LOADING CONFIGURATION :

Analysis of the 3-D boundary loading conditions at the hip joint have been performed by Paul (1967), Johnston, Brand & Crowninshield (1978). The minimum function at the hip joint is that required for the activities of daily living to be performed. An acceptable function means the ability to walk on the level, up and down slopes and up and down steps, and to sit down and stand up with little or no use of the arms. Among these activities of foremost importance is walking and so the loading configuration for walking activity is considered in the analysis.

The experimental results of the hip joint loading have been used in finite element studies of the human femur. Rybicki et. al.,(1972) [ref.14] cosidered a hip joint load of 169 lbf (= 751.7 N) in one-legged stance for a body weight of 200 lb (= 889.6 N). He has estimated the hip abductor muscle force to be 358 lbf (1592.4 N) and thereby increased the joint load on the femoral head to 521 lbf (2317.4 N). The abductor muscle force was assumed to be produced by only the gluteus medius and gluteus minimus muscles.

Andriacchi et. al.,[ref.15] performed a 2-D stress analysis of the femoral stem of a total hip prostheses considering normalized joint load (1N) applied to the femoral head in the three directions (0,20,45) degrees with respect to the longitudinal axis of the femoral stem.

Svensson et. al.,[ref.10] used the results of Mcleish and Charnley(1970) to perform the 2-D stress analysis of the femur with implanted Charnley prostheses. They have taken a joint load of 1620 Newtons (2.35 times body weight) at 24.3 degrees with the femoral shaft and the trochanter load of 1062 Newtons (1.54 times body weight) at 29.5 degrees with the femoral shaft in the one-legged stance activity.

Sih & Matic [ref.16] considered the abductor muscle force as a shearing force acting on the greater trochanter and distributed joint load over the femoral head in their 2-D analysis for the failure prediction of the total hip prosthesis system. They have taken a joint load of 960 Newtons distributed over 60 degrees arc on the femoral head and a shearing traction 7.10E5 Pascals on the greater trochanter for a 444.8 Newtons body weight in one-legged stance.

Crowninshield et. al.,[ref.17,18] presented a detailed analysis of the loading at the hip joint considering the effect of 27 separate musculo- tendinous units. However, his attention is mainly on the acetabular component and the loads cannot be transfered to the femoral head without the prior knowledge of the orientation of the loads with respect to the femoral head.

Paul's results [ref.19,20] of the loading on the femoral head are best suited for the present study. Paul

has simplified the complex anatomical system of 22 muscles acting at the hip and 14 muscles and 6 ligaments at the knee to groups on their anatomical disposition and, for the muscles, on the basis of their phasic activity as demonstrated by myoelectric signals. On this simplified basis the variation of the hip joint force (as multiples of body weight) is evaluated for a walking cycle activity for slow, normal and fast walking corresponding to 1.10, 1.48 and 2.01 M/S average forward speed. The results are shown in figure 8. The maximum force on the femoral head occurs at 47% of the cycle time from heel strike and its magnitude is 4.9 times body weight in slow and normal walking, and 7.6 times body weight in fast walking. The orientation of the maximum force from the axis joining the centre of the femoral head to the centre of the condyle is shown to be 12.5 degrees in the frontal view and 7 degrees in the lateral view [figure 9]. Paul also showed the maximum joint force in stairs ascending to be 7.2 times body weight and in stairs descending to be 7.1 times body weight. Also the maximum force while climbing up the ramp is 5.9 times body weight and descending down the ramp is 5.1 times body weight.

In the present study the results for the walking cycle activity, as mentioned above, are chosen from Paul's work. Since the exact geometric location of the joint load is uncertain and since the load is transmitted to the

femoral cup through the contact area of the acetabular cup therefore the maximum load is considered to be distributed over an appropriate small region on the femoral head rather than considering it to be applied to a single node. Taking the body weight to be 660 Newtons, the load on the femoral head is taken to be

4.9 X 660 = 3234 Newtons for slow & normal walking

7.6 X 660 = 5016 Newtons for fast walking.

The angle of inclination of the femoral cup from the axis joining the centre of the femoral head to the centre of the condyle is 48 degrees on the average[ref.20]. Therefore the inclination of the maximum load on the femoral head is 35.5 (= 48-12.5) degrees from the surface replacement cup axis[figure 10]. Considering the joint load orientation to be along the 35.5 degree axis a contact region of 50 degree arc, i.e., 25 degree arc on either side of the load axis, is arbitrarily selected as shown in figure 10.

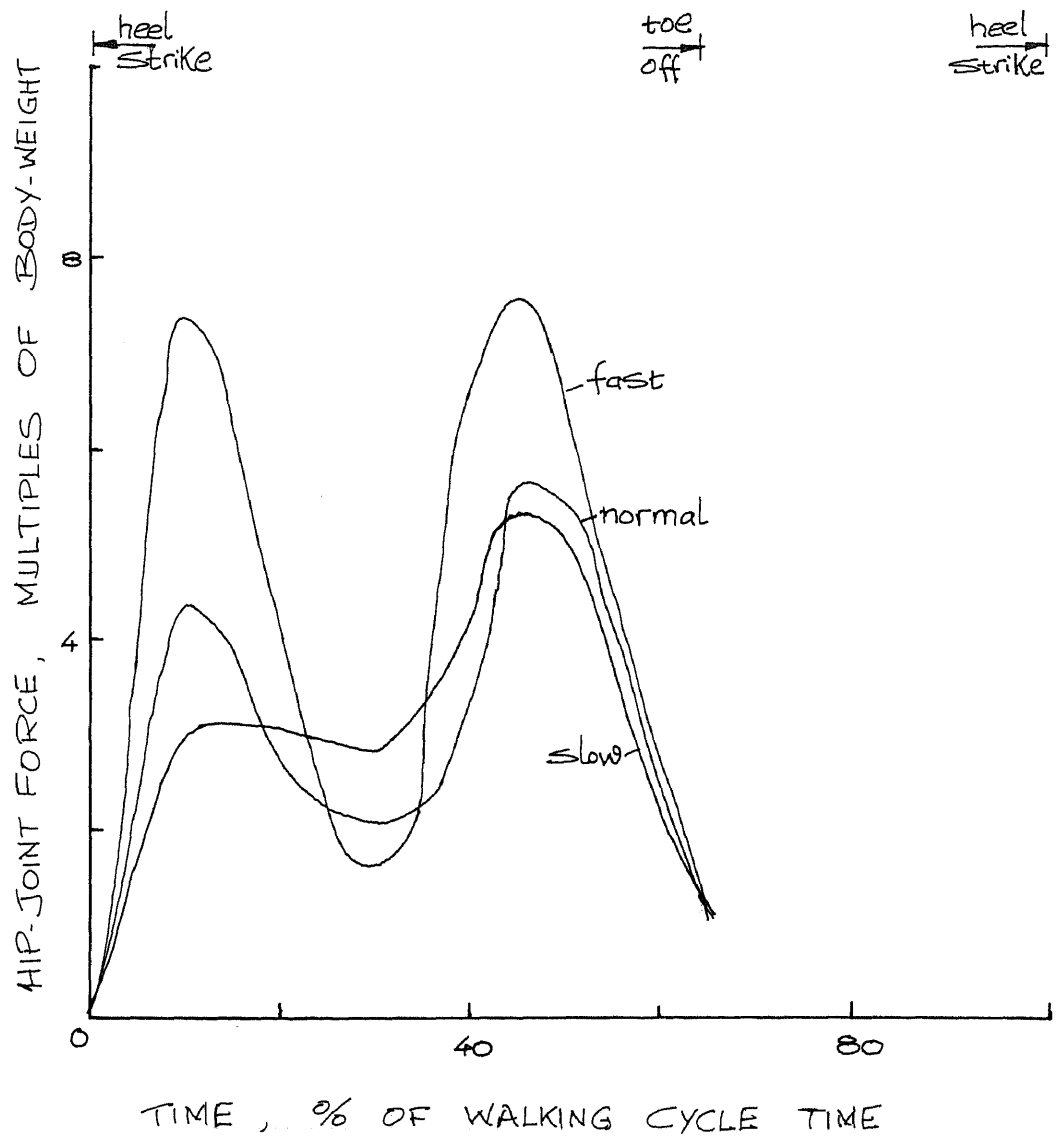

HIP JOINT LOAD FOR WALKING CYCLE	REF. 19,20
	FIGURE 8

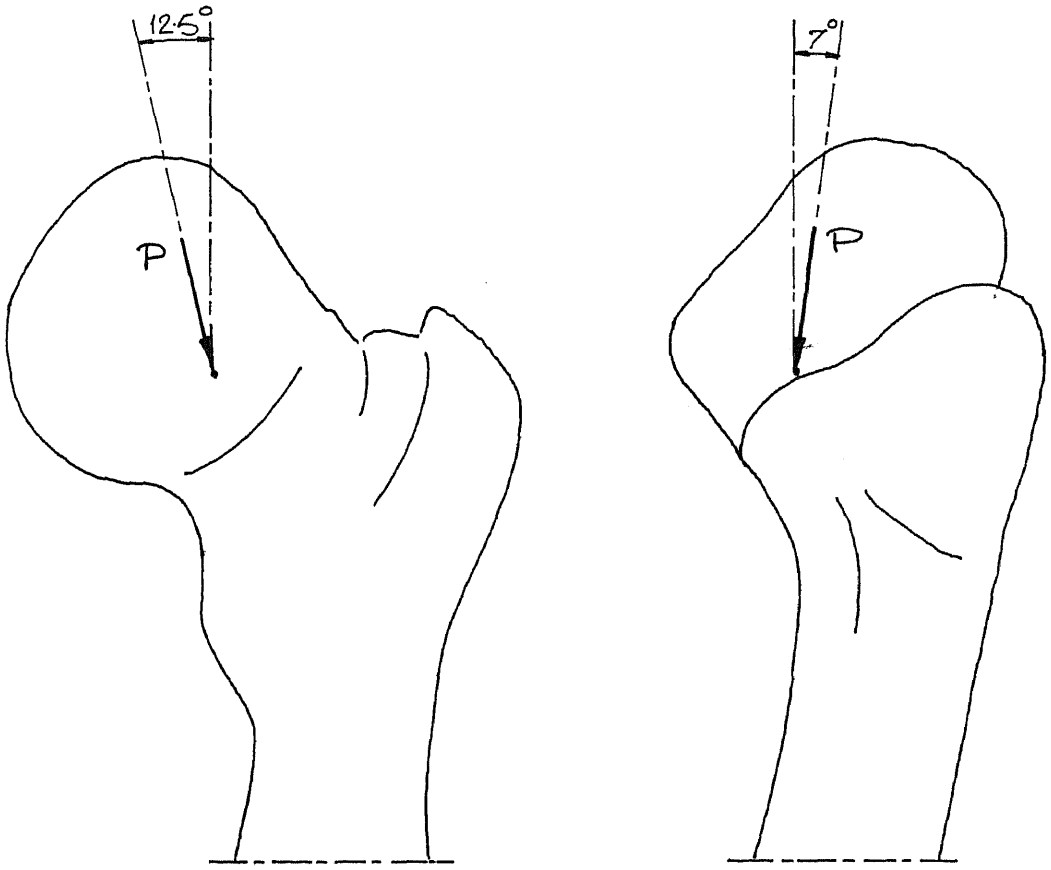

MAXIMUM LOAD (AT 47% CYCLE TIME)

ORIENTATION OF MAX. LOAD ON FEMORAL HEAD FOR WALKING	REF. 19,20
	FIGURE 9

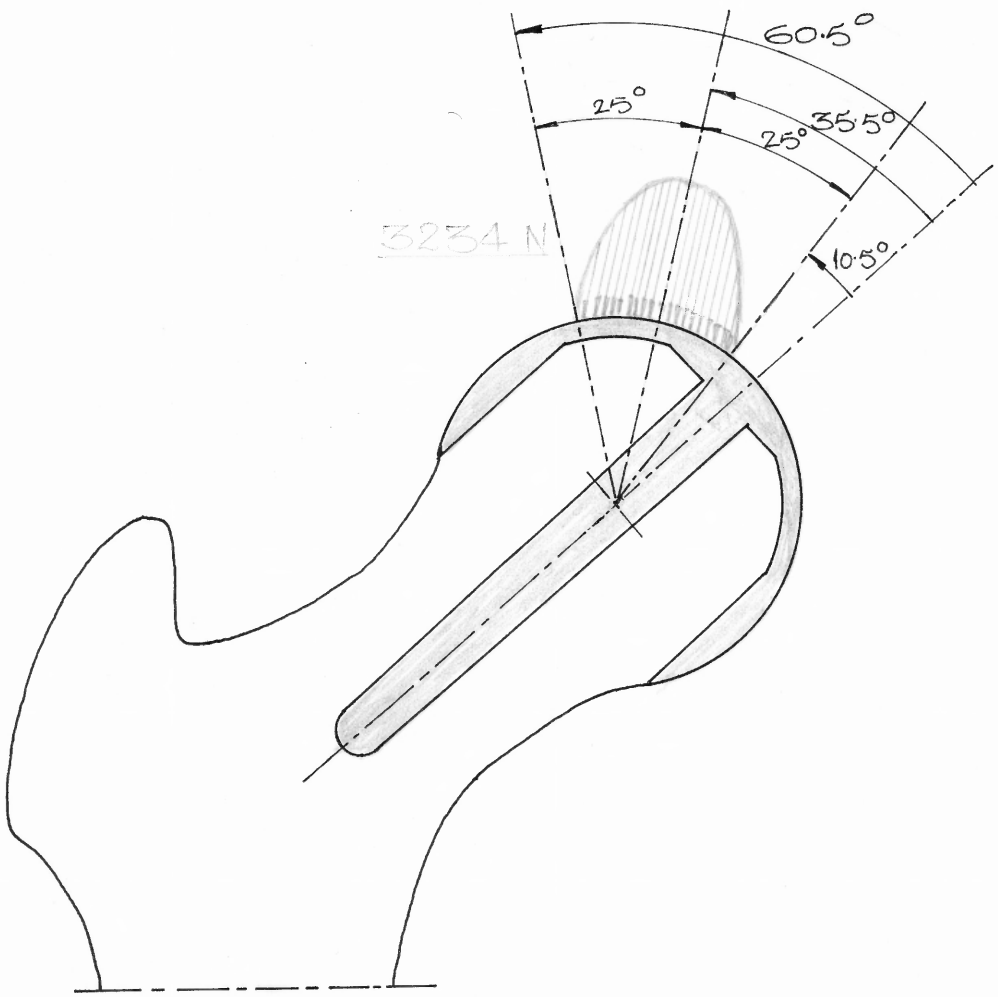

SELECTED LOADING ON THE FEMORAL HEAD	REF. 19,20
	FIGURE 10

7) THE FINITE ELEMENT MODEL OF THE FEMORAL CUP

The finite element analysis is done by constructing the model using quadratic displacement, linear strain elements namely TA6 and QA9 elements supported by GIFTS 5.06. Considerable improvements can be obtained with this higher order element mesh generation as compared to that with 2-D constant strain elements. The elements, TA6 and QA9, schematically shown in figure 11, are used in axisymmetric solid problems for accurate determination of displacements and stresses.

The model under study consists of the femoral head with its surface replaced by a metal cup shown in figure 13. The size and shape of the metal cup is clearly shown in figure 12. According to St. Venant's principle the region "far away" from the application of loads is unaffected and so the length of the model considered ranges from the head to the proximity of the neck. The model is generated using the mesh generation capabilities of GIFTS software. The mesh of the elements generated is shown in figure 11. Since the stresses at the prostheses- cement- bone interface are of importance therefore a finer mesh is generated in the interfacial region. The details of mesh generation is presented in the following section.

The model is subdivided into different regions based upon the variation of the material properties. In the ideal

case the material properties are truly axisymmetric. However, since the bone properties vary with growth considering adults with different ages, therefore the regions are chosen by judgement representing very closely the variation of material properties presented by Brown et al.,[ref.8,13]. By suitable interpolation and averaging methods the material properties for the different regions are chosen and are tabulated in table IV. The bone properties chosen are as follows[ref. table II]:

Young's modulus : 1300 - 7900 MPa

Yield strength : 62 - 262 MPa

Poisson's ratio : 0.37 - 0.42

The material properties of the acrylic cement are taken as follows[ref.10]:

Young's modulus : 2070 MPa

Ultimate strength: 69.9 MPa

Poisson's ratio : 0.19

The material chosen for the metal cup is the standard ASTM-F75, surgical cobalt chromium alloy and its properties are as follows:

Young's modulus : 196100 MPa

Ultimate strength : 650 MPa

Poisson's ratio : 0.30

Each of the regions, selected on the basis of the variation of material properties is subdivided into elements as follows - all quadrilateral regions are meshed with quadrilateral QA9 elements and all triangular regions are meshed with triangular TA6 elements. In all there are 10 regions defined using 44 keynodes leading to 198 quadrilateral displacement, linear strain elements. The external loading on the model is considered for walking cycle activity from Paul's results[ref.19,20]. As mentioned earlier a load of 3234 Newtons is chosen for slow and normal walking and a load of 5016 Newtons is chosen for fast walking. This loading is distributed on the curve 3-4-5 [ref.figure 15].

Symmetric boundary conditions are applied to the model along the axis 35-44 [cf. figure 15], i.e., the nodes along this axis have the x-translational degree of freedom suppressed. The nodes along the bottom edge, i.e., 10-44 [cf. figure 15] are held rigid considering the end-condition. To facilitate the sliding connection between the axial rod of the metal cup and the adjacent bone, the nodes along the edge, i.e., 20-33-43 [cf.figure 15] have only the y-translational degree of freedom.

With the above information the model is generated, analyzed and the resulting stresses at the interfacial

region are obtained. As mentioned earlier the iterative finite element stress analyses are performed by appropriate variation of the stiffness, in relation to the stresses, in the prostheses- bone region till the desired conversence is achieved.

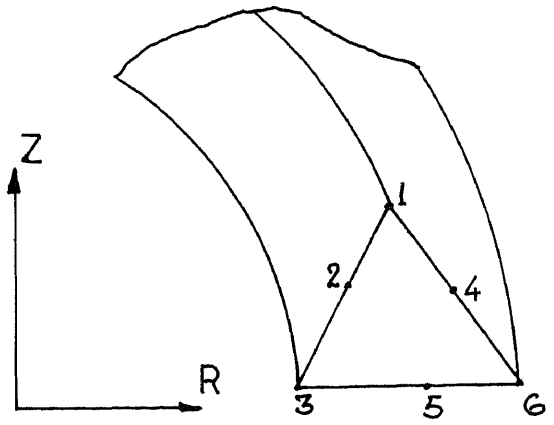

LINEAR STRAIN AXISYMMETRIC TRIANGLE TA6

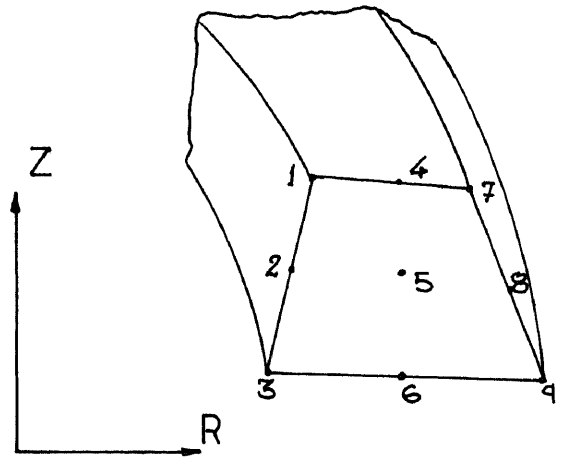

LINEAR STRAIN AXISYMMETRIC QUADRILATERAL QA9

TA6 & QA9 ELEMENTS	REF. 22
	FIGURE 11

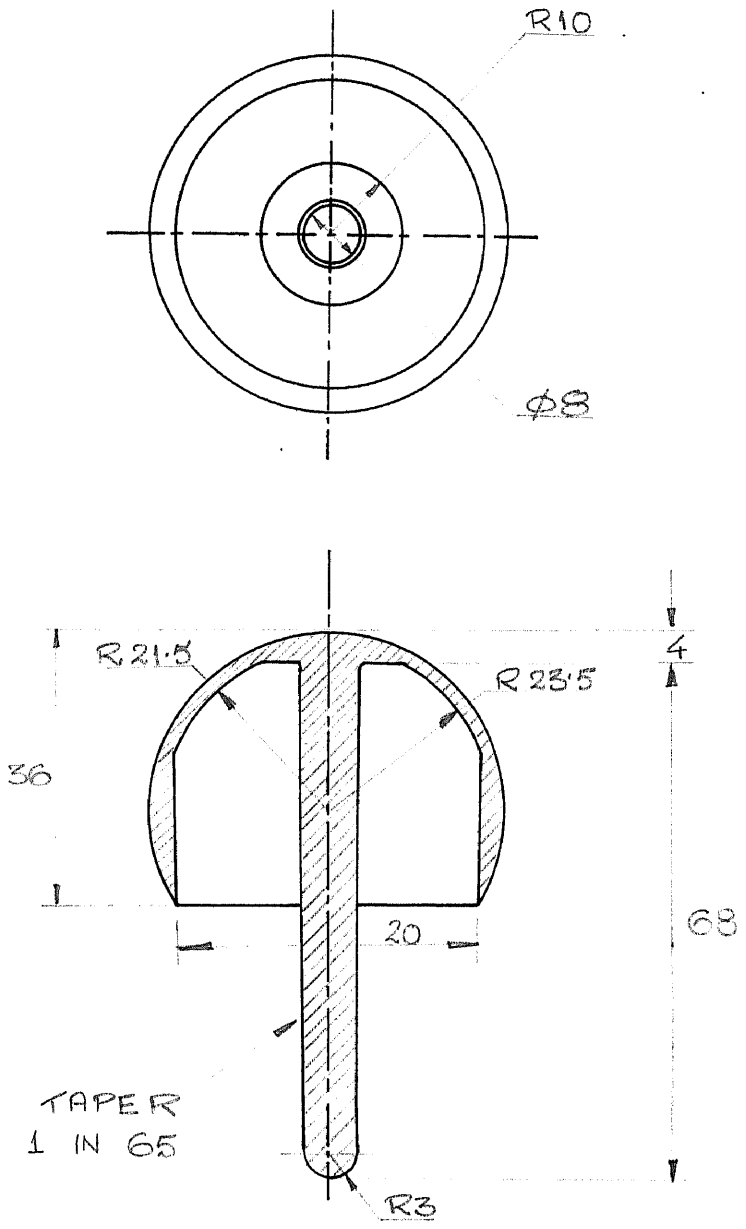

ALL DIMENSIONS IN MM.
REF. NO. 21

EXTERNAL CUP DIMENSIONS

SCALE 1:1

FIGURE 12

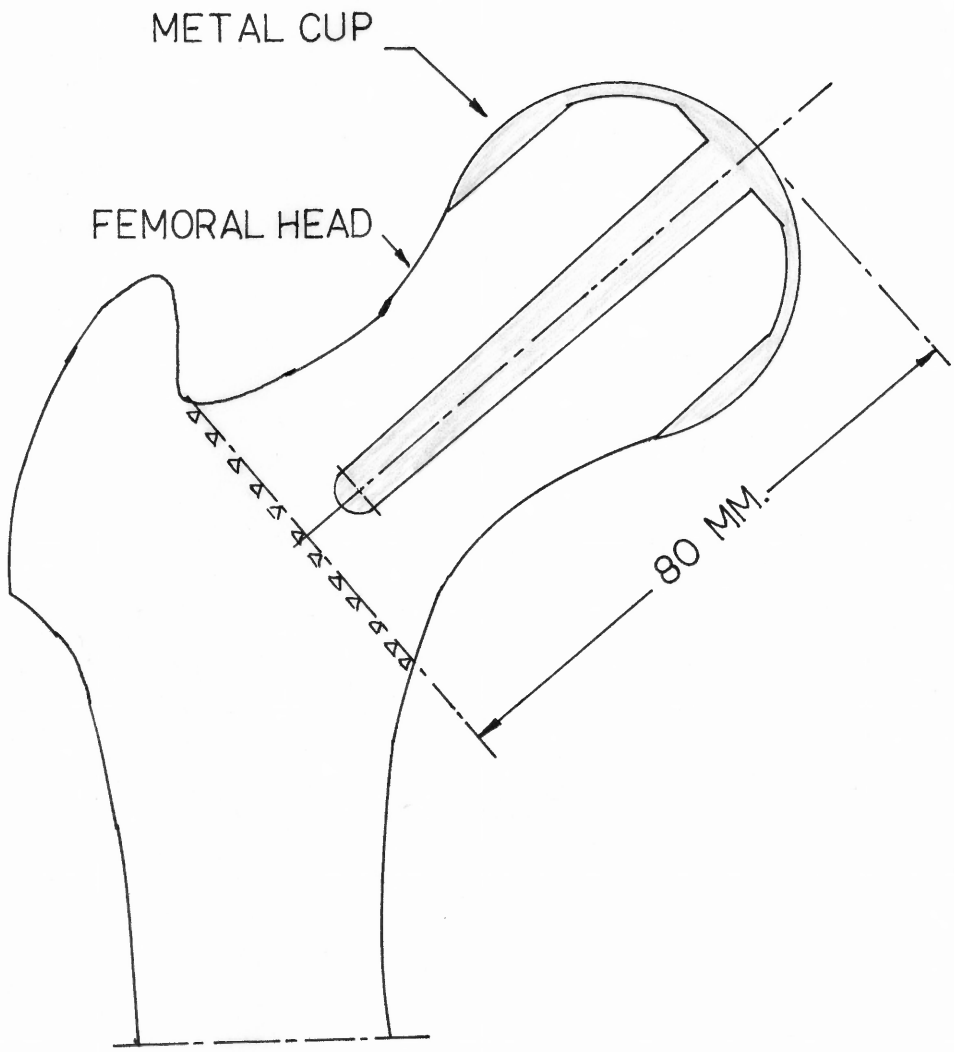

AXISYMMETRIC MODEL OF THE FEMORAL HEAD

SCALE 1:1

FIGURE 13

8) ANALYSIS USING GIFTS 5.06 :

The analysis using the GIFTS software typically consists of the execution of the following modules in sequence[ref.22]:

BULKM/EDITM - to generate the model ,

BULKF/BULKLB/EDITLB - to generate the loadings as a series of sine-cosine harmonic functions ,

OPTIM - to optimize the bandwidth ,

STIFFX - to compute the stiffness matrix for the axisymmetric model,

SAVEK - to store the stiffness matrix for later use,

SOLAX - to compute the displacements ,

STRESX - to compute the stresses ,

RESULTS - to display the results , eg, stress contours in the model.

9) MESH GENERATION USING GIFTS 5.06

The model generation is performed using the mesh generator module BULKM. Due to the axisymmetric conditions only one half of the structure need to be modelled (cf. fig 14). The process of mesh generation is carried out in the following steps :

1) define material & thickness menu,

2) define key points,

3) define line & curve boundaries, and finally

4) define grids.

In the present case there are 7 distinct "material properties" sets defined for the regions as given in table IV. Each material property set consists of the Young's modulus, E, the Poisson's ratio, μ, and the design stress, S_y. The later is used as a reference to compare the computed stresses.

Material properties are defined using the commands,

```
ELMAT,3      ( define  the first 3 prop. )
1            ( set identifier # 1 )
1.E4,1.E7,0.3  ( set # 1 properties : Sy,E,μ )
2            (set identifier # 2)
---- ---- ---
3
---- ---- ---
```

and so on for all the 7 sets.

The grid generation proceeds as follows. The 2-D surface of the model is divided into several regions each having 3 or 4 sides based on the following criterion. Each pair of opposite sides of the quadrilateral region have same number of nodes and all the sides of the sides of the triangular region must have same number of nodes. The grid boundaries may be defined by straight lines, circular arcs or 2nd or 3rd order parametric curves. With this preliminary work the key nodes can be defined at the corners of the grids. The key points and the regions selected for the present study are labelled in figure 14.

The key nodes 1 to 46 are defined by the user with the following commands:

```
KPOINT      ( generate one or more key nodes )
46           ( key node # 46 )
0.,0.,0.    ( x46,y46,z46 )
10           ( key node # 10 )
22.5,0.,0.  ( x10,y10,z10 )

and so on

0           ( terminate key node input )
```

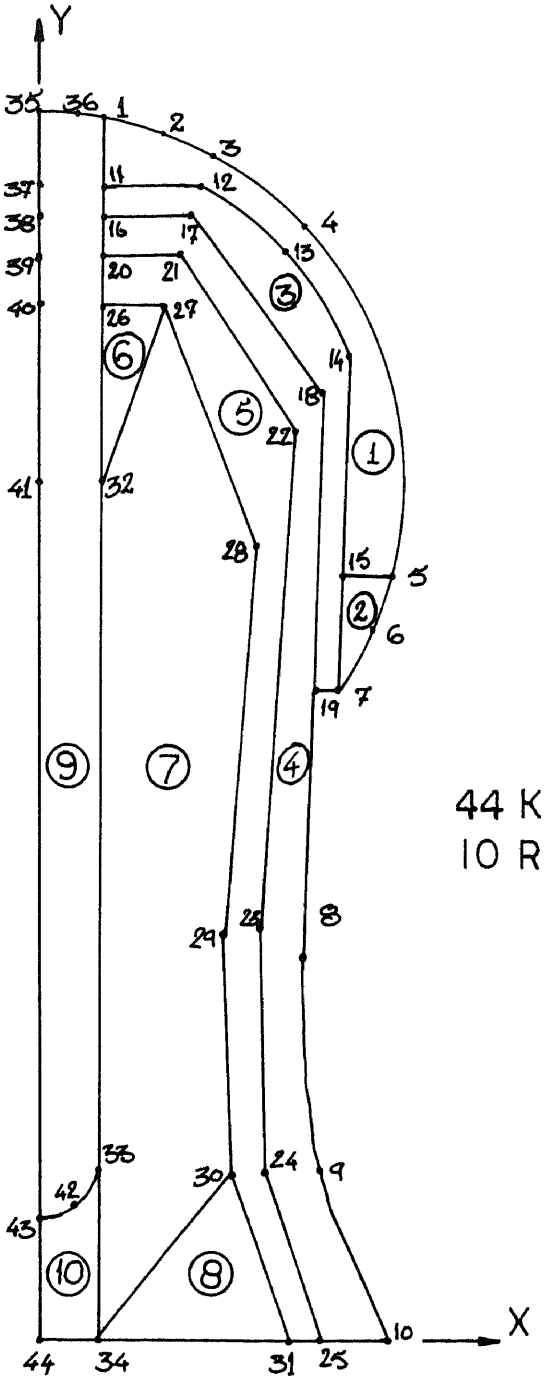

KEY NODES AND REGIONS OF THE MODEL

SCALE 2:1

FIGURE 14

TABLE III. USER DEFINED KEY NODE CO-ORDINATES

KEYNODE	X-COORD	Y-COORD	Z-COORD	KEYNODE	X-COORD	Y-COORD	Z-COORD
1	4.0	79.5	0.0	23	14.5	27.5	0.0
2	7.5	78.0	0.0	24	14.5	33.0	0.0
3	11.0	77.0	0.0	25	17.5	0.0	0.0
4	22.0	66.0	0.0	26	4.0	68.0	0.0
5	24.0	51.0	0.0	27	7.5	68.0	0.0
6	22.5	47.0	0.0	28	14.0	54.5	0.0
7	20.0	44.0	0.0	29	12.0	26.5	0.0
8	17.5	28.0	0.0	30	12.0	11.5	0.0
9	17.5	11.5	0.0	31	15.5	0.0	0.0
10	22.5	0.0	0.0	32	0.0	56.5	0.0
11	4.0	76.0	0.0	33	3.0	12.0	0.0
12	10.0	76.0	0.0	34	3.0	0.0	0.0
13	16.5	71.5	0.0	35	0.0	80.0	0.0
14	20.0	51.0	0.0	36	2.0	79.25	0.0
15	20.0	51.0	0.0	37	0.0	76.0	0.0
16	4.0	73.5	0.0	38	0.0	73.5	0.0
17	9.5	73.5	0.0	39	0.0	71.0	0.0
18	19.0	62.0	0.0	40	0.0	68.0	0.0
19	18.5	44.0	0.0	41	0.0	56.5	0.0
20	4.0	71.0	0.0	42	0.88	8.88	0.0
21	8.5	71.0	0.0	43	0.0	8.0	0.0
22	16.75	59.0	0.0	44	0.0	0.0	0.0

TABLE IV. MATERIAL PROPERTIES OF THE REGIONS

REGION #	YOUNGS MODULUS,E (Newtons/ sq. mm)	YIELD STRENGTH, (Newtons/ sq. mm)	POISSON's RATIO
1	196100	650(*)	0.30
2	196100	650(*)	0.30
3	2070	69.9(*)	0.19
4	7900	262	0.42
5	6600	193	0.37
6	6600	193	0.37
7	3900	131	0.37
8	5100	143	0.37
9	196100	650(*)	0.30
10	1300	62	0.37

Regions # 1,2 & 9 represent the metal cup

Region # 3 represents the acrylic cement

Note: (*) - based on ultimate strength(ref.10)

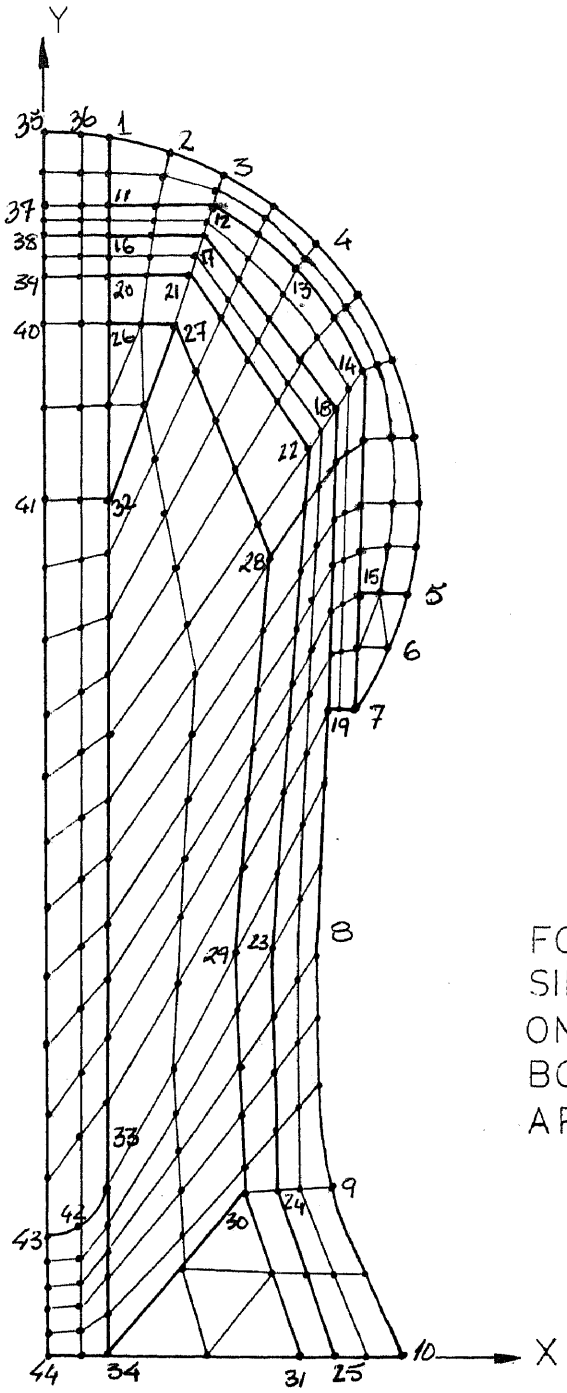

FOR
SIMPLICITY
ONLY
BOUNDARY PTS.
ARE SHOWN

THE COMPLETE MODEL

SCALE 2:1

FIGURE 15

The user defined key node co-ordinates are presented in table III. Once the key nodes have been defined the next step is to generate curves which define the boundaries of the 10 regions considered. Since the metal cup is spherical in shape therefore the curves between the key nodes, representing the metal cup are generated as circular arcs (cf. fig 14). The curve 8-9-10 on the cortical bone surface is taken to be a 2nd order parametric curve.

Along with the generation of the curves the other internal nodes are defined to enable subdivision of each region into TA6 and QA9 type elements. The generation of these internal nodes is considered uniform without any biasing. The total number of nodes considered on these curves should suffise the generation of the elements later on. To generate straight lines two key nodes are sufficient but to generate circular or parametric curves three nodes are necessary.

Straight line curves are generated using the instruction SLINE. A straight line curve named 'L1025' between nodes 10 and 25 and having 3 intermediate nodes on it can be generated as follows:

```
SLINE
L1025       ( curve identifier )
10,25,5     ( end key nodes are 10,25  and
              total # of nodes= 5)
```

Likewise circular arcs are generated using the instruction CARC and the 2nd order parametric curves using the instruction PARAM2.

For example ,

```
CARC      (to generate circular arc)
C57     (curve identifier)
5,6,7,5   (key nodes are 5,6,7 and
           total # of nodes= 5)

PARAM2    (to generate param2 arc)
L810      (curve identifier)
8,9,10,11 (key nodes are 8,9,10 and
           total # of nodes = 11)
```

The followins instructions generate all the curves which will be used to define the regions.

```
CARC/ C351/ 35,36,1,5//   (generate circular arc 'C351'
                          with nodes 35,36 & 1 and total #
                          of nodes on the curve is 5)

CARC/ C13/ 1,2,3,5//

CARC/C35 /3,4,5,17//

CARC/ C57/5,6,7,5//

PARAM2/ L810/ 8,9,10,11//

SLINE/ L198/ 19,8,7//  (generate st. line 'L198'
                        between nodes 19 & 8 with a
                        total of 7 nodes)

SLINE/ L1112/ 11,12,5//
```

```
SLINE/ L1415/ 14,15,9//
SLINE/ L155/ 15,5,5//
CARC/ C1214/ 12,13,14,9//
SLINE/ L715/ 15,7,5//
SLINE/ L1617/ 16,17,5//
SLINE/ L1718/ 17,18,9//
SLINE/ L1819/ 18,19,13//
SLINE/ L197/ 19,7,5//
SLINE/ 2122/ 21,22,9//
SLINE/ L2021/ 20,21,5//
SLINE/ L2223/ 22,23,17//
SLINE/ L2324/ 23,24,9//
SLINE/ L2425/ 24,25,5//
SLINE/ L2526/ 25,26,9//
SLINE/ L2627/ 26,27,5//
SLINE/ L2829/ 28,29,13//
SLINE/ L2930/ 29,30,11//
SLINE/ L3031/ 30,31,5//
SLINE/ L3034/ 30,34,5//
SLINE/ L3233/ 32,33,23//
SLINE/ L4143/ 41,43,23//
SLINE/ L3334/ 33,34,11//
CARC/ C3343/ 33,42,43,5//
SLINE/ L1025/ 10,25,5//
SLINE/ L2531/ 25,31,3//
SLINE/ L3134/ 31,34,5//
```

```
SLINE/ L3444/ 34,44,5//
SLINE/ L4344/ 43,44,11//
SLINE/ L1116/ 11,16,5//
SLINE/ L1620/ 16,20,5//
SLINE/ L2026/ 20,26,3//
SLINE/ L2632/ 26,32,5//
SLINE/ L3227/ 32,27,5//
SLINE/ L3537/ 35,37,5//
SLINE/ L3738/ 37,38,5//
SLINE/ L3839/ 38,39,5//
SLINE/ L3940/ 39,40,3//
SLINE/ L4041/ 40,41,5//
SLINE/ L111/ 1,11,5//
```

Once the curves have been generated some of these can be combined together into simple curves, to help define the grid boundaries, using the COMPLINE command which is defined as follows:

```
COMPLINE
NAME
L1,L2,...
```

The above instructions define the composite line 'NAME', composed of lines 'L1', 'L2', etc. A maximum of 9 lines can be combined into a composite. None of the component lines may themselves be composites.

The followins instructions define the combined boundary curves used in the model seneration:

```
COMPLINE/ B15/ C13,C35//
COMPLINE/ B1115/ L1112,C1214,L1415//
COMPLINE/ B117/ L1112,L1214, L1415,L157 //
COMPLINE/ B1619/ L1617,L1718,L1819//
COMPLINE/ B2025/ L2021,L2122,L2223, L2324,L2425//
COMPLINE/ B1610/ L1617,L1718,L1819, L198,L810//
COMPLINE/ B2631/ L2627,L2728,L2829, L2930,L3031 //
COMPLINE/ B2730/ L2728,L2829, L2930//
COMPLINE/ B3234/ L3233,L3334 //
COMPLINE/ B133/ L111,L1116,L1620, L2026,L2632,L3233 //
COMPLINE/ B3543/ L3537,L3738,L3839, L3940,L4041,L4143 //
```

The followins curves are senerated to ease the application of symmetry and boundary conditions (applied in the module BULKLB).

```
COMPLINE/ L1044/ L1025,L2531, L3134,L3444//
COMPLINE/ L2033/ L2026,L2632,L3233 //
COMPLINE/ L3544/ L3537,L3738,L3839, L3940,L4041,L4143, L4344//
```

After definins the srid boundaries the last step in the model seneration is the seneration of the srid elements. The instruction GETY allows one to define the

element type, material number and thickness number for the surface elements to be generated in a particular region (grid). The number of nodes on each of the edges have been previously chosen so as to enable the generation of the higher order elements. A four sided grid is generated by the command GRID4 and a three sided grid is generated by the command GRID3.

Necessary precautions should be taken when generating elements by automatic mesh generation to avoid highly distorted elements which lead to poor numerical results. So in order to avoid numerical inaccuracies, all TA6 elements should have no angles less than 15 degrees or greater than 150 degrees and also the ratio between any two sides should not be greater than 4. Likewise for QA9 elements the ratio of any two sides should not be greater than 4 and any vertex angle should not be smaller than 15 degrees or greater than 150 degrees.

The followins instructions enable the generation of TA6 elements in a 3- sided grid, say region 2 :

```
GETY
TA6          (element type)
1,1          ( defines mat. set # and thickness set #)
GRID3
G2           (grid identifier)
L155,C57,L715  (boundary curves identifiers)
```

Likewise the following instructions are used to generate QA9 elements in a 4- sided grid, say region 5:

```
GETY
QA9          (element type)
4,1          (mat. set # 4 and thickness set # 1)
GRID4
G5           (grid identifier)
L2026,B2631, L2531,B2025  (boundary curve id's)
```

The following instructions are used to generate the grid elements:

```
GETY/QA9/1,1// GRID4/G1/ B15,L155,B1115,L111 //
GETY/TA6/1,1// GRID3/G2/ L155,C57,L715 //
GETY/QA9/2,1// GRID4/G3/ L1116,B1621, L197,B117 //
GETY/QA9/3,1// GRID4/G4/ L1620,B2025, L1025,B1610 //
GETY/QA9/4,1// GRID4/G5/ L2026,B2631, L2531,B2025 //
GETY/TA6/4,1// GRID3/G6/ L2627,L2632,L3227 //
GETY/QA9/5,1// GRID4/G7/ L3227,B2730, L3034,B3234 //
GETY/TA6/6,1// GRID3/G8/ L3034,L3134,L3031 //
GETY/QA9/1,1// GRID4/G9/ C351,B133, C3343,B3543 //
GETY/QA9/7,1// GRID4/G10/ C3343,L4344, L3444,L3334 //
```

The model with the grid boundaries can be plotted

using the module BULKM. However, to plot the generated elements the module EDITM has to be used. The finite element model as a whole is shown in figure 15.

Once the model has been generated the next step is to define the boundary loading conditions for the model using the modules BULKLB and EDITLB. BULKLB can be used to apply distributed line and surface loads onto the model generated by BULKM. The solution of multiple load cases is permitted in the GIFTS system. Commands for suppressing and releasing degrees of freedom are at the user's disposal. Loads to keynodes and grid boundaries can be applied using commands LOADK and LOADL in the module BULKLB. However, loads to any of the system nodes can be applied using the command LOADP in the module EDITLB. The loading configuration for this analysis is taken from Paul's results [ref.19,20] for a walking cycle activity.

The module BULKF is executed before BULKLB to generate the freedom pattern for the model. BULKF allows only those freedoms which the model can support and thus relieves the user of the necessity of suppressing all superflous freedoms by hand.

Distributed line load can be applied using the command LOADL, which is defined as follows:

LOADL,M	Line load in M direction
LNAME	Curve identifier
V1,V2	End values of the load

M = 1,2,3 for force along X,Y,Z directions respectively.

The distributed loading on the femoral head considered is R= 3234 Newtons along the arc approximately from 10.5 to 60.5 degrees from the cup axis. The arc length of the loading is obtained as follows:

Arc Length, S = radius X subtended angle

= 40 X (50 X 3.1415/ 180)

= 34.91 mm.

The horizontal component of the loadings at the arc extremes is

V1 = (3234 / 34.91) * SIN (10.5 degrees)

= 16.88 Newtons

V2 = (3234 / 34.91) * SIN (60.5 degrees)

= 80.63 Newtons

Similarly the vertical component of the loadings at the two ends is

V1 = (3234 / 34.91) * COS (10.5 degrees)

= 91.09 Newtons

V2 = (3234 / 34.91) * COS (60.5 degrees)

= 45.62 Newtons

The above loadings is applied using the commands:

LOADL,1 loadings in X- dir.

C35 curve identifier

-16.88,-80.63 end-values of the load

```
LOADL,2       loadins in Y- dir.
C35             curve identifier
-91.09,-45.62  end-values of the load
```

The freedom pattern can be modified for all nodes alons a line usins the commands SUPL and RELL which are defined as follows:

```
    SUPL (,M)        suppresses freedom M in all nodes
    LNAME            of the line LNAME
```

If M = 0 then all freedoms are suppressed.

```
    RELL (,M)        releases freedom M in all nodes
    LNAME            of the line LNAME
```

If M= 0 then all freedoms are released.

The nodes alons the edse 10-44 (cf. fis.15) are held risid applyins the end condition bu the command,

```
SUPL,0/ L1044 //
```

The nodes alons the edse 35-44 have x- translational desree of freedom suppressed bu the symmetru condition. This is accomplished usins the command

```
SUPL,1 / L3544 //
```

To facilitate the slidins connection the nodes alons the boundaru curve 20-33-43 have all desrees of freedom

suppressed except for the y- translational c
freedom. The followins commands are used to perm.
slidins connection.

```
SUPL,0 / L2033 //
RELL,2 / L2033 //
SUPL,0 / C3343 //
RELL,2 / C3343 //
```

This completes the mesh seneration application of boundary conditions. The model solved on executins the modules OPTIM, STIFFX, and STRESX respectively in sequence. The stress analysis can be obtained from the moc

10) REFERENCES

1) Pellicci,P.M., Salvati,E.A., and Robinson,H.J., "Mechanical Failures in Total Hip Replacement requiring reoperation", The Journal of Bone and Joint Surgery, vol.61-A, No.1, January 1979, pp28-36.

2) Beckenbaugh,R.D., and Ilstrup,D.M., "Total Hip Arthroplasty", The Journal of Bone and Joint Surgery, vol.60-A, No.3, April 1978, pp306-313.

3) Amstutz,H.C., Graff-Radford,A., Gruen,T.A., and Clarke,I.C., "Tharies Surface Replacements", Clinical Orthropaedics and Related Research", vol.134, 1978, pp87-101.

4) Koch,J.C., "The laws of bone architecture", American Journal of Anatomy, vol.21, 1917, pp177-298.

5) Rao,S.S., "The finite element method in engineering", Persamon Press Ltd., New York, 1982.

6) Bathe,K.J., "Finite element procedures in engineering analysis", Prentice-Hall, Inc., Englewood Cliffs, N.J., 1982.

7) Clarke,I.C., Gruen,T.A., Tarr, and Sarmiento, International Conference proceedings on finite elements in Biomechanics, february 1980.

8) Brown,T.D., and Ferguson,A.B., "The development of a computational stress analysis of the femoral head", The Journal of Bone and Joint Surgery, vol.60-A, No.5, July

1978, pp619-629.

9) Crowninshield,R.D., Brand,R.A., and Johnsto
"Analysis of femoral stem design in tota
arrthroplasty", Transactions of the Orthopaedic
Society, February 1979, p33.

10) Svensson,N.C., Valliappan,S., and Wood,R.D
analysis of human femur with implanted
prosthesis", Journal of Biomechanics, vol
pp581-588.

11) Van Buskirk,W.C., Cowin,S.C., Ward,R.N., "U
measurement of orthotropic elastic constants
femoral bone", Journal of Biomechanical
vol.103, 1981, pp67-72.

12) Valliappan,S., KJellbers,S., and
International Conference Proceedings on fini
Biomechanics, February 1980.

13) Brown,T.D., and Graf,G.E., "Mate
distributions in the human femoral head",
the Orthopaedic Research Society, vol.3:15,

14) Rybicki,E.F., Simonen,F.A., and Weis,I
mathematical analysis of stress in the
Journal of Biomechanics, vol.5,1972, pp203-215.

15) Andriacchi,T.P., Galante,J.O., Belytschko
Hampton,S., "A stress analysis of the femoral
hip prostheses", The Journal of Bone and
vol.58-A, No.5, July1976, pp618-624.

16) Sih,G.C., and Matic,P., "Failure prediction of the total hip prosthesis system", Journal of Biomechanics, vol.14, 1981, pp833-841.

17) Crowninshield,R.D., Johnston,R.C., Andrews,J.G., and Brand,R.A., "A Biomechanical investisation of the human hip", Journal of Biomechanics, vol.11, 1978, pp75-85.

18) Johnston,R.C., Brand,R.A., Crowninshield,R.D., "Reconstruction of the hip", The Journal of Bone and Joint Surgery, vol.61-A, No.5, July 1979, pp639-652.

19) Paul,J.P., "Load actions on the human femur in walkins and some resultant stresses", Experimental Mechanics, vol.11, March 1971, pp121-125.

20) Paul,J.P., "Force actions transmitted by Joints in the human body", Proceedinss of the Royal Society, London, vol.B192, 1976, pp163-172.

21) Pappas,M., "Femoral component, N.J. Conservative Hip", Endomedics Incorporation, Part# SRH-003.

22) Kamel,H.A., McCabe,M.W., and Hunten,K.A., The GIFTS system, Version 5.03 User's Reference Manual, April 1981, Univ. of Arizona, Tucson, Arizona.